JOURNAL OF SOLID STATE CHEMISTRY 35, 376–384 (1980)

Chemical Diffusion in Intermediate Phases in the Lithium–Tin System

C. JOHN WEN AND ROBERT A. HUGGINS

Department of Materials Science and Engineering, Stanford University, Stanford, California 94305

Received January 7, 1980; in revised form March 12, 1980

The compositional variation of the chemical diffusion coefficient in the six intermediate phases LiSn, Li_7Sn_3, Li_5Sn_2, $Li_{13}Sn_5$, Li_7Sn_2, and $Li_{22}Sn_5$ of the lithium–tin system at 415°C has been measured. Among these intermediate phases, the phase $Li_{13}Sn_5$ has the highest chemical diffusion coefficient, varying with composition from 5.01×10^{-5} to 7.59×10^{-4} cm²/sec at that temperature. Combining this information with coulometric titration curves (emf versus composition), the self-diffusion coefficient of lithium has also been determined in the various intermetallic phases as a function of composition under the assumption that the tin atoms do not move appreciably compared with the lithium atoms. The lithium self-diffusion coefficient in the phase LiSn is lower than those in the more lithium-rich phases by one order of magnitude. This result is discussed in terms of the difference between the crystal structures of LiSn and the other lithium-rich phases in the lithium–tin system.

Introduction

In the development of advanced lithium alloy/metal-sulfide high-performance secondary batteries, investigations of the compositional variations of thermodynamic and transport properties of solid lithium alloys are urgently needed. Such studies can help understand and evaluate the performance of solid lithium alloys as active materials in negative electrodes. Because of the scarcity of data on the lithium chemical potential and chemical diffusion coefficient in solid lithium alloys, a systematic study of a number of lithium alloy systems has been undertaken. Such experimental results not only provide thermodynamic and kinetic information about the specific systems, but also furnish guidelines for searching for new lithium alloys as negative electrode materials.

A prior thermodynamic study of the lithium–tin system at temperatures from 360 to 590°C has revealed that there are six intermediate phases (*1*). The nominal compositions are LiSn, Li_7Sn_3, Li_5Sn_2, $Li_{13}Sn_5$, Li_7Sn_2, and $Li_{22}Sn_5$, respectively. In addition, since the only X-ray diffraction pattern available in the ASTM standard file relating to these phases is that for $Li_{22}Sn_5$, powder diffraction patterns of all the phases have also been investigated (*2*).

This paper reports experimental determinations of the compositional dependence of the emf versus pure lithium, the thermodynamic enhancement factor, the chemical diffusion coefficient, and the lithium self-diffusion coefficient within all six of these phases.

Experimental Procedures

The electrochemical measurements were

0022-4596/80/150376-09$02.00/0

made using a three-electrode cell of the type

$$\text{Al,“LiAl”}|\text{LiCl–KCl (eut.)}|\text{Li}_y\text{Sn}, \quad \text{(I)}$$

where Li_ySn represents the solid lithium–tin phases under investigation, Al,“LiAl” denotes the two-phase mixture of lithium—aluminum with a composition of about 40 a/o Li. This mixture was used as both the lithium activity reference electrode and as the lithium-reservoir counter electrode. The LiCl–KCl eutectic molten salt was used as the electrolyte. It was obtained from Lithcoa. An alumina crucible was employed as the container for the molten salt. The lithium–tin sample electrode, reference, and counter electrodes were all suspended within the salt from the top. Molydenum has been shown to be suitable for use as the electrical lead material at all lithium activities (*2–5*). In addition, the solubility of lithium in molybdenum is negligibly small at the temperature of these experiments (*6*). This cell was heated in a simple 6-in. high resistance furnace. The entire experimental setup was installed in a controlled atmosphere glove box (Vacuum/Atmosphere Co.) filled with recycling helium gas. The concentrations of water vapor, oxygen, and nitrogen gas were maintained below about 1 ppm.

A detailed description of the preparation of the two-phase lithium–aluminum reference and counter electrodes has been given elsewhere (*1*). The emf of the two-phase Al, “LiAl” reference electrode relative to pure lithium is about 300 mV at 415°C, and its dependence upon temperature has been reported by several investigators (*5, 7–9*). The eutectic mixture of LiCl and KCl was heated in an alumina crucible at 420°C for about 12 hrs before use. Without further treatment these molten salts were clear and colorless.

The various solid lithium–tin phases used in the diffusion measurements were prepared by melting the preweighed amounts of lithium (99.9%, Foote Mineral) and tin (99.9%, Baker) metals of the nominal stoichiometric compositions in molybdenum cups with lids at temperatures from 525 to 825°C inside the glove box. The alloys were annealed at 450°C for about 12 hrs and then they were allowed to cool to room temperature in several hours. The alloys were crushed and ground to powder in a porcelain mortar with a pestle in the glove box. The powder was sieved to 150 mesh and cold pressed into pellets of $\frac{3}{8}$-in. diameter at a pressure of 90,000 psi under a helium atmosphere. A molybdenum sheet was wrapped around the pellet to prevent the circumference from being directly exposed to the electrolyte. As a result, one-dimensional diffusion into the sample from the two planar sides could be assumed.

The electrochemical measurements were made using either a PAR 173 potentiostat/galvanostat with a plug-in PAR 179 digital coulometer or an Aardvark PEC-1 potentiostat in conjunction with a free-standing PAR 379 digital coulometer. Directly measured open-circuit voltages indicated that some of the alloys prepared by this fusion technique were not in the desired single-phase regions, and this suggested that there was a slight loss of lithium, possibly due to evaporation during the preparation process. In all cases, the proper composition was assured by applying a constant voltage, corresponding to the known single-phase composition determined by direct coulometric titration of lithium into pure tin, between the working electrode and the two-phase Al,“LiAl” reference electrode until the current became negligibly small. It usually took less than half an hour to reach such a steady-state composition for all phases except for LiSn, which required a longer time for equilibration.

After the sample electrode attained a uniform composition a small voltage step (4 to 8 mV) was imposed and the transient

current, $I(t)$, was monitored as a function of time, t. The chemical diffusion coefficient, $\tilde{D}$, was evaluated from the long-time approximation for a potentiostatic experiment as (*7*)

$$I(t) = \frac{2Q\tilde{D}}{L^2} \exp\left(-\frac{\pi^2\tilde{D}t}{4L^2}\right), \quad \text{if } t \gg L^2/\tilde{D}, \quad (1)$$

where L, Q, and S were the half-thickness of the sample pellet, the total charge transferred as a result of the voltage step, and the total surface area common to both the working electrode and the electrolyte phase, respectively. The total charge, Q, accumulated in a given voltage interval, ΔE, was also used to obtain the coulometric titration curve or emf versus composition data. The change in composition expressed in terms of deviations from the ideal stoichiometry, δ, for the lithium–tin phase $Li_{a+\delta}Sn_b$ was calculated according to Faraday's law with the assumption of 100% coulombic efficiency, i.e., $\Delta\delta = bQ/Fn_{Sn}$, where n_{Sn} was the number of moles of tin and F the Faraday constant. The magnitude of n_{Sn} was calculated from the weight and the original composition of the alloy sample.

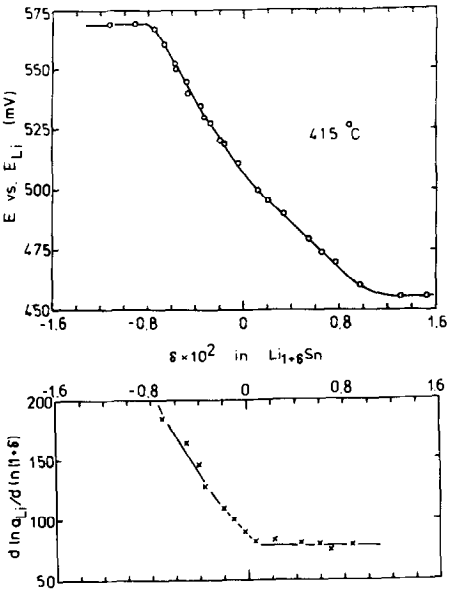

FIG. 1. Coulometric titration curve (top) and the compositional variation of the thermodynamic enhancement factor (bottom) within the phase LiSn.

Results

Phase LiSn

Above 360°C LiSn has been shown to be the most tin-rich phase in the lithium–tin system (*1*). Figure 1 presents the measured open-circuit voltage and the calculated thermodynamic enhancement factor as functions of composition at 415°C. This phase is stable between 569 and 456 mV with respect to pure lithium at 415°C. The homogeneity range expressed in terms of stoichiometric parameter, $\Delta\delta$, is 1.7×10^{-2}. The thermodynamic enhancement factor for a single-phase lithium–tin phase $Li_{a+\delta}Sn_b$ was evaluated according to the expression (*3*)

$$\frac{d \ln a_{Li}}{d \ln(a+\delta)} = -\frac{F}{RT}(a+\delta)\frac{dE}{d\delta} \simeq -\frac{aF^2 n_{Sn}\Delta E}{bRTQ}, \quad (2)$$

where a_{Li}, R, T, and ΔE are the lithium activity, the gas constant, the absolute temperature, and the applied voltage step, respectively. It is interesting to note that the compositional dependence of the thermodynamic enhancement factor is similar to that of the "LiAl" phase in the lithium–aluminum system (*7*). It is essentially constant with a value of 80 in the region of positive deviations from the ideal stoichiometry, but increases with decreasing lithium concentration on the lithium-poor side of LiSn, reaching a value of about 185 near the tin-rich phase boundary.

Figure 2 shows the compositional variations of the chemical diffusion coefficient and the lithium self-diffusion coefficient in

the phase LiSn. Within that phase's stability range, the chemical diffusion coefficient varies from 2.24×10^{-6} to 4.10×10^{-6} cm²/sec, and shows a minimum at (or near) the nominal stoichiometric composition. The self-diffusion coefficient of lithium in $Li_{a+\delta}Sn_b$ was calculated by use of the expression

$$\tilde{D} = D_{Li}\left(\frac{d \ln a_{Li}}{d \ln(a + \delta)}\right). \quad (3)$$

The quantity in the bracket on the right-hand side of this expression is the thermodynamic enhancement factor, which is related to the thermodynamic nonideality of the alloy phase and generally assumes values larger than unity. The self-diffusion coefficient of lithium describes the random motion of lithium atoms in the absence of a chemical concentration gradient. The above equation is directly related to the Darken equation (*10*), with the assumption that the tin atoms do not move appreciably. In contrast to the chemical diffusion coefficient, the lithium self-diffusion coefficient in the phase LiSn shows a monotonic increase in value from 2.03×10^{-8} to 4.16×10^{-8} cm²/sec as more lithium is added.

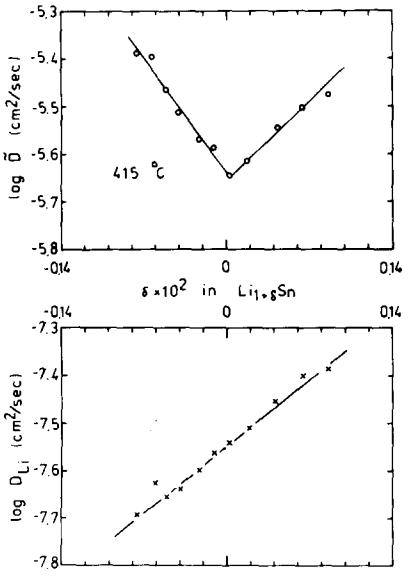

FIG. 2. Compositional variation of the chemical diffusion coefficient (top) and the lithium self-diffusion coefficient (bottom) within the phase LiSn.

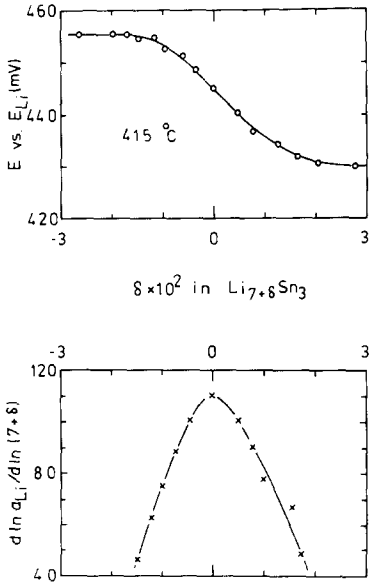

FIG. 3. Coulometric titration curve (top) and the compositional variation of the thermodynamic enhancement factor (bottom) within the phase Li_7Sn_3.

The open-circuit voltage and the calculated thermodynamic enhancement factor are shown in Fig. 3 as functions of composition within the phase Li_7Sn_3. The coulometric titration curve shows an inflection point right at the nominal composition. The emf of phase Li_7Sn_3 lies between 456 and 430 mV relative to pure lithium, corresponding to a lithium activity variation from 4.57×10^{-4} at $\delta = -1.5 \times 10^{-2}$ to 7.08×10^{-4} at $\delta = 2.0 \times 10^{-2}$. The experimental data on the thermodynamic enhancement factor show that it varies from 46 to 110 over the existence range, with a maximum at the nominal stoichiometric composition.

Figure 4 shows the chemical diffusion coefficient and lithium self-diffusion coefficient as functions of composition for the phase Li_7Sn_3. The compositional behavior of the chemical diffusion coefficient, which varies from 2.57×10^{-5} to $4.07 \times$

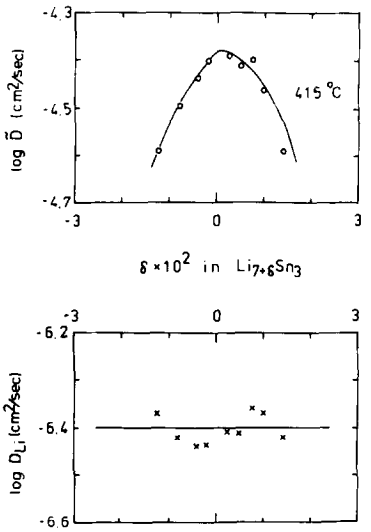

FIG. 4. Compositional variation of the chemical diffusion coefficient (top) and the lithium self-diffusion coefficient (bottom) within the phase Li_7Sn_3.

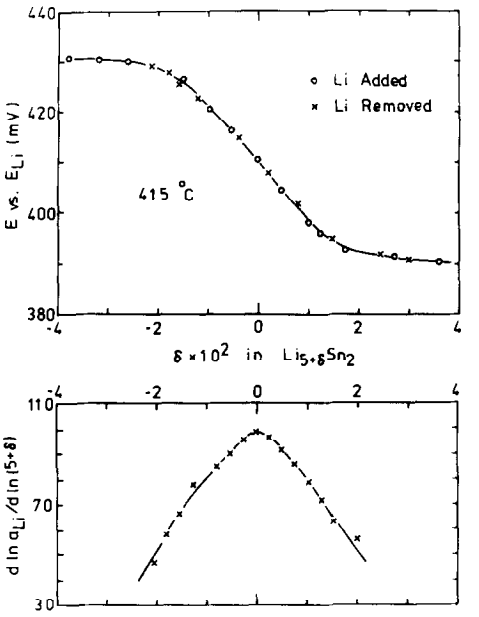

FIG. 5. Coulometric titration curve (top) and the compositional variation of the thermodynamic enhancement factor (bottom) within the phase Li_5Sn_2.

10^{-5} cm²/sec, closely resembles that of the thermodynamic enhancement factor. On the other hand, the self-diffusion coefficient of lithium in Li_7Sn_3 is nearly independent of composition, with an average value of 3.98 $\times$ 10^{-7} cm²/sec.

In Fig. 5, the emf and the thermodynamic enhancement factor in the phase Li_5Sn_2 are plotted as functions of composition. The coulometric titration curve indicates that the data obtained by adding lithium to the sample electrode correspond very well with those determined by removing lithium from the sample electrode. As in the case of phase Li_7Sn_3, the emf versus composition data yield a symmetrical curve with an inflection point at the nominal composition, where the thermodynamic enhancement factor also shows a maximum. The range of emf is from 430 to 390 mV relative to pure lithium over the composition range from $\delta = -3 \times 10^{-2}$ to $\delta = 3 \times 10^{-2}$ at 415°C. The values of the thermodynamic enhancement factor are seen to vary from 33 to 99.

The variation of the chemical diffusion coefficient in the phase Li_5Sn_2 with respect to composition is similar to that of the thermodynamic enhancement factor, as shown in Fig. 6. The chemical diffusion

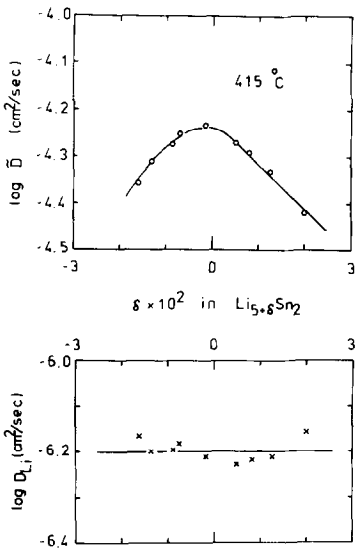

FIG. 6. Compositional variation of the chemical diffusion coefficient (top) and the lithium self-diffusion coefficient (bottom) within the phase Li_5Sn_2.

coefficient increases from 3.89×10^{-5} cm²/sec at $\delta = 2 \times 10^{-2}$ to a maximum value of 5.89×10^{-5} cm²/sec at the nominal stoichiometric composition as the lithium concentration decreases, and then decreases with decreasing lithium concentration. However, the lithium self-diffusion coefficient in Li_5Sn_2 is nearly composition independent, with a mean value of 6.31×10^{-7} cm²/sec.

Phase $Li_{13}Sn_5$

As shown in Fig. 7, the open-circuit voltage relative to pure Li varies gradually with composition in the region of negative deviations from the nominal stoichiometry in the phase $Li_{13}Sn_5$, but drops more rapidly on the lithium-rich side. At 415°C, this emf value decreases from 390 mV at about $\delta = -4 \times 10^{-2}$ to 286 mV at $\delta = 2.5 \times 10^{-2}$. Figure 7 also shows that the thermodynamic enhancement factor increases by three orders of magnitude with increasing lithium concentration, reaching a maximum

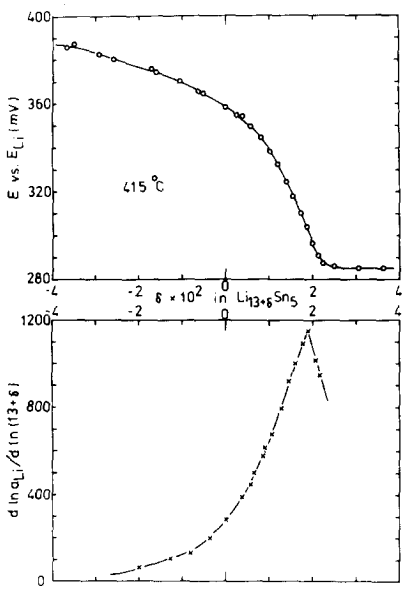

FIG. 7. Coulometric titration curve (top) and the compositional variation of the thermodynamic enhancement factor (bottom) within the phase $Li_{13}Sn_5$.

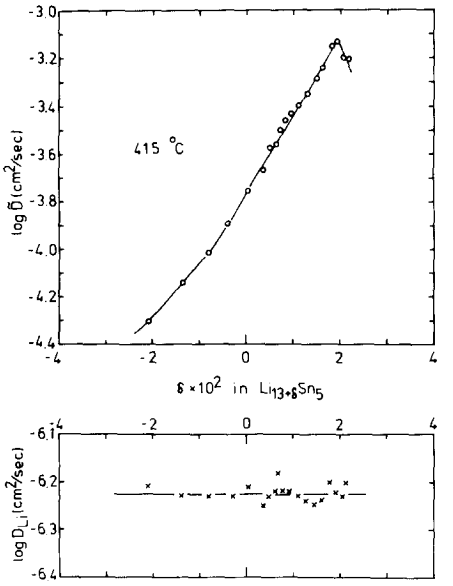

FIG. 8. Compositional variation of the chemical diffusion coefficient (top) and the lithium self-diffusion coefficient (bottom) within the phase $Li_{13}Sn_5$.

value of 1150 at $\delta = 1.9 \times 10^{-2}$. Thereafter, it decreases somewhat as even more lithium is added.

The compositional dependence of the chemical diffusion coefficient in phase $Li_{13}Sn_5$ is very similar to that of the thermodynamic enhancement factor. As shown in Fig. 8, the chemical diffusion coefficient varies from 5.01×10^{-5} to 7.59×10^{-4} cm²/sec. The self-diffusion coefficient of lithium in $Li_{13}Sn_5$, however, is essentially constant, with an average value of 5.96×10^{-7} cm²/sec at 415°C.

Phase Li_7Sn_2

As shown in Fig. 9, a plot of emf versus composition yields an almost symmetrical curve with an inflection point near the nominal stoichiometric composition of Li_7Sn_2. The open-circuit voltage varies from 280 mV at $\delta = -5.0 \times 10^{-2}$ to 170 mV at $\delta = 5.0 \times 10^{-2}$ versus pure lithium. The thermodynamic enhancement factor varies from 128 to 196, with a maximum at the nominal stoichiometry.

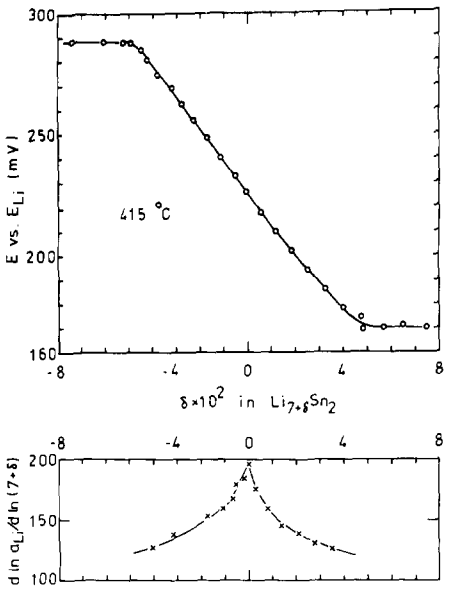

FIG. 9. Coulometric titration curve (top) and the compositional variation of the thermodynamic enhancement factor (bottom) within the phase Li_7Sn_2.

In Fig. 10, the chemical diffusion coefficient within the Li_7Sn_2 phase is shown to have a maximum at or near the nominal stoichiometric composition, where its value is 7.76×10^{-5} cm²/sec. The lithium self-diffusion coefficient in Li_7Sn_2 is essentially composition independent, with a mean value of 4.47×10^{-7} cm²/sec at 415°C.

Phase $Li_{22}Sn_5$

$Li_{22}Sn_5$ is the most lithium-rich intermediate phase in the lithium–tin system (*1, 17*). The measured open-circuit voltage was found to slowly drift with time at high lithium activities. The total charge, Q, used in the calculation of the change in composition, $\Delta\delta$, for each voltage step was the arithmetric mean of experiments run in the two opposite directions. The value of Q was further checked by the following expression

$$Q = \frac{\pi^2 I_0}{8k}, \tag{4}$$

where I_0 and k were the extrapolated intercept at $t = 0$, and the slope of a linear plot of $\ln I$ versus t, i.e., Eq. (1) or the long-term expression for the transient current $I(t)$ as a function of time, t, in a potentiostatic experiment.

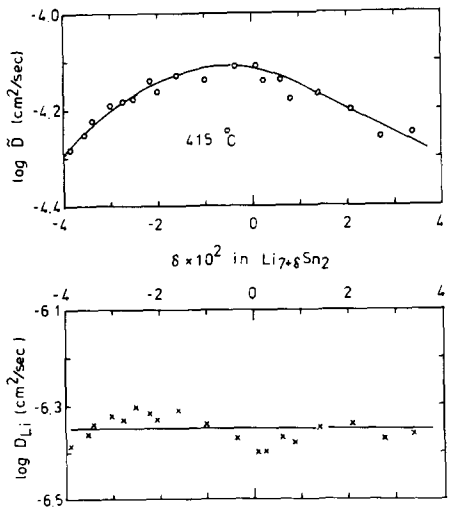

FIG. 10. Compositional variation of the chemical diffusion coefficient (top) and the lithium self-diffusion coefficient (bottom) within the phase Li_7Sn_2.

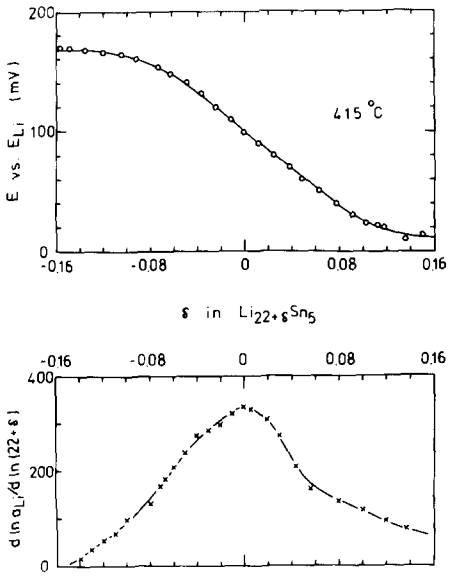

FIG. 11. Coulometric titration curve (top) and the compositional variation of the thermodynamic enhancement factor (bottom) within the phase $Li_{22}Sn_5$.

The thermodynamic data for the $Li_{22}Sn_5$ phase are given in Fig. 11. The emf relative to pure lithium decreases in value from 170 mV at $\delta = -0.15$ to 10 mV at $\delta = 0.15$, following a slightly asymmetrical curve with an inflection point near the nominal stoichiometric composition, similar to those of Li_7Sn_3, Li_5Sn_2, and Li_7Sn_2, as shown in previous sections. The thermodynamic enhancement factor ranges from 18 to 335, with a maximum at the nominal stoichiometric composition.

The transport properties of the $Li_{22}Sn_5$ phase are shown in Fig. 12. The chemical diffusion coefficient, which varies from 6.58 $\times$ 10^{-5} to 1.91 $\times$ 10^{-4} cm^2/sec, shows a maximum near the nominal stoichiometric composition. The self-diffusion coefficient of lithium within the phase $Li_{22}Sn_5$ is seen to vary with composition in the range of $\delta = -0.03$ to $\delta = 0.05$. However, it appears to be essentially independent of composition for $\delta > 0.05$ or $\delta < -0.03$. The constant values of the lithium self-diffusion coefficient are 9.12 $\times$ 10^{-7} and 4.79 $\times$ 10^{-7} cm^2/sec on the lithium-rich side and lithium-poor side of the composition range, respectively.

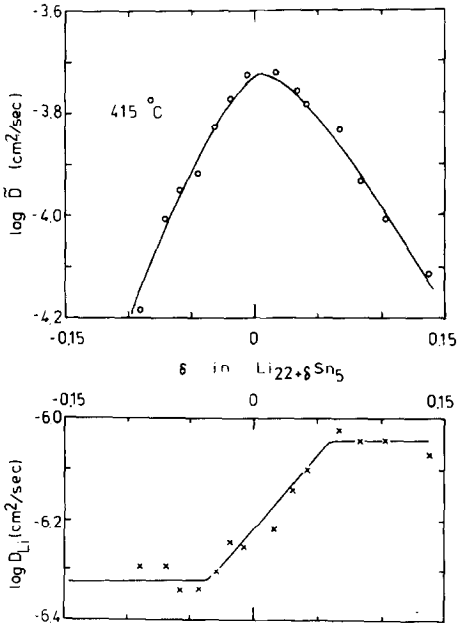

FIG. 12. Compositional variation of the chemical diffusion coefficient (top) and the lithium self-diffusion coefficient (bottom) within the phase $Li_{22}Sn_5$.

Discussion

The ranges of the chemical diffusion coefficients, the self-diffusion coefficients, and the thermodynamic enhancement factors (TEF) across all of the intermediate phases in the lithium–tin system at 415°C are presented in Table I. Although all the phases have reasonably high chemical diffusion coefficients, the phase $Li_{13}Sn_5$ has the largest value, approaching 10^{-3} cm^2/sec. This is higher than the chemical diffusion coefficients in most liquids by about two orders of magnitude. This extremely high value within the phase $Li_{13}Sn_5$ can be seen to be related to the large value of the thermodynamic enhancement factor, of the order 10^3.

As evident in Table I, the lithium self-diffusion coefficients in phases Li_7Sn_3, Li_5Sn_2, $Li_{13}Sn_5$, Li_7Sn_2, and $Li_{22}Sn_5$ are all of the same order of magnitude. On the other hand, the lithium self-diffusion coefficient in LiSn is about one order of magnitude lower. This interesting result may be discussed in terms of the differences in the crystal structure of LiSn from those of the more lithium-rich phases.

TABLE I

THERMODYNAMIC AND KINETIC DATA FOR INTERMEDIATE PHASES IN THE LITHIUM–TIN SYSTEM

Phase	TEF	D (cm^2/sec)	D_{Li} (cm^2/sec)
LiSn	80–185	2.24–4.10 $\times$ 10^{-6}	2.03–4.16 $\times$ 10^{-6}
Li_7Sn_3	46–110	2.57–4.07 $\times$ 10^{-5}	3.63–4.37 $\times$ 10^{-7}
Li_5Sn_2	33–99	3.89–5.89 $\times$ 10^{-5}	5.89–6.92 $\times$ 10^{-7}
$Li_{13}Sn_5$	18–1150	5.01–75.9 $\times$ 10^{-5}	5.62–6.61 $\times$ 10^{-7}
Li_7Sn_2	128–196	4.90–7.76 $\times$ 10^{-5}	3.89–5.01 $\times$ 10^{-7}
$Li_{22}Sn_5$	18–335	6.58–19.1 $\times$ 10^{-5}	4.79–9.12 $\times$ 10^{-7}

The structures of all the other intermediate phases are based on a *bcc* packing characterized by 14-fold coordination of nearest and next-nearest neighbors (*11*). According to Frank and Kasper (*12*), for a *bcc* structure the coordination number of an icosahedron is 14, rather than 8. As in the case of the intermediate phases in the lithium–lead system (*13–16*), the five phases in the lithium–tin system have basically the same type *bcc* packing as lithium metal, but with the appropriate fraction of lithium atoms replaced by tin atoms in such a way as to regularly distribute the tin atoms among the available sites.

The crystal structure of the phase LiSn is a variant of *bcc* packing. Each atom is surrounded by eight opposite atoms and four like atoms (*16*). Thus, the coordination number is 12. This is different from the other lithium-rich intermediate phases, which all have a 14-fold coordination. This difference in crystal structures between LiSn and the other more lithium-rich phases is surely related to the observation that the self-diffusion coefficients of lithium in LiSn is one order of magnitude smaller than it is in the other phases.

Acknowledgment

This work was supported by the U.S. Department of Energy under Contract EC-77-S-02-4506 and LBL Subcontract 4503110.

References

1. C. JOHN WEN AND R. A. HUGGINS, *J. Electrochem. Soc.*, in press (1981).
2. C. JOHN WEN, Ph. D. dissertation, Stanford University, 1980.
3. W. WEPPNER AND R. A. HUGGINS, *J. Electrochem. Soc.* **124,** 1569 (1977).
4. W. WEPPNER AND R. A. HUGGINS, *J. Solid State Chem.* **22,** 297 (1977).
5. WEPPNER AND R. A. HUGGINS, *J. Electrochem. Soc.* **125,** 7 (1978).
6. F. A. SHUNK, "Constitution of Binary Alloys," p. 479, 2nd Suppl., McGraw–Hill, New York (1969).
7. C. JOHN WEN, W. WEPPNER, B. A. BOUKAMP, AND R. A. HUGGINS, *J. Electrochem. Soc.* **126,** 2258 (1979).
8. N. P. YAO, L. A. HEREDY, AND R. C. SAUNDERS, *J. Electrochem. Soc.* **118,** 1039 (1971).
9. R. A. SHARMA AND R. N. SEEFURTH, *J. Electrochem. Soc.* **123,** 1763 (1976).
10. L. S. DARKEN, *Trans. AIME* **175,** 184 (1948).
11. U. FRANK AND W. MULLER, *Z. Naturforsch. B* **30,** 316 (1975).
12. F. C. FRANK AND J. S. KASPER, *Acta Crystallogr.* **11,** 184 (1958).
13. A. ZALKIN AND W. J. RAMSEY, *J. Phys. Chem.* **62,** 689 (1958).
14. A. ZALKIN AND W. J. RAMSEY, *J. Phys. Chem.* **60,** 234 (1956).
15. A. ZALKIN, W. J. RAMSEY, AND D. H. TEMPLETON, *J. Phys. Chem.* **60,** 1275 (1956).
16. A. ZALKIN AND W. J. RAMSEY, *J. Phys. Chem.* **61,** 1413 (1957).
17. W. MULLER AND H. SCHAFER, *Z. Naturforsch. B* **28,** 246 (1973).